INVERSE DESIGN OF INTERNALLY COOLED TURBINE BLADES BASED ON THE HEAT ADJOINT EQUATION

INVERSE DESIGN OF INTERNALLY COOLED TURBINE BLADES BASED ON THE HEAT ADJOINT EQUATION

Michele Ferlauto
Mechanical and Aerospace Engineering Dept., Politecnico di Torino
Corso Duca degli Abruzzi 24, 10129 Torino, Italy.
e-mail *: michele.ferlauto@polito.it*

[1]

Abstract

A method of solution of the inverse problem in heat conduction is presented. The method, based on an adjoint optimization procedure, is applied to the design of the pattern of circular cooling passages inside coated turbine blades. The general case of a non-homogeneous solid material is considered. The numerical solution of both the temperature field and of the adjoint problem is based on a finite element method. The mathematical method is explained and the procedure is validated against theoretical and experimental data available in open literature.

Keywords. Inverse problem, heat conduction, adjoint methods.

1 Introduction

A wide range of engineering problems in thermal analysis and design has been formulated as inverse heat transfer problems [1]. The inverse problem involves the estimation of the cause by utilizing the knowledge of the effect. Several studies focus on the relation cause-effect between heat flux and temperature. A classical example of this class of inverse problems deals with the estimation of an unknown boundary heat flux, by using temperature measurements taken below the boundary surface. Other studies estimate the steady or unsteady inlet temperature profile, or cover aero-thermal effects by estimating steady/transient wall heat flux in laminar flow, or deduce inlet velocity estimation based on the temperature measurements. For conciseness, the interested reader is addressed to [1, 2, 3, 4, 5, 6] and references therein. In fact, the abovementioned problems are out of the scope of the present work, which belongs to the class of the design problems.
The design problem can be formulated as an inverse problem in which some conditions are given at the boundary, while the shape of the body contour that realizes the imposed thermal features is unknown. Applications of this approach to heat conduction design problems have been proposed and successfully applied to turbine blade cooling in the last three decades. The heat conduction inverse problem of design the geometry of the internal cooling passages of a turbine blade has been solved for circular [8], super-elliptic [10], generic geometries of the cooling passages in multi-holed turbine blade [7, 9]. The numerical procedures are based mainly on a direct solver driven by an optimization method. In one of the earliest applications [8] a Boundary Element Method (BEM) for heat conduction analysis and a gradient method, the Steepest Descent Method (SDM), have

[1]Please send correspondence to:
Michele Ferlauto
Dept. of Mechanical and Aerospace Engineering, Politecnico di Torino
c.so Duca degli Abruzzi, 24 - 10129 Torino, Italy
phone: +39 011 0906834
telefax: +39 011 0906899
e-mail*: michele.ferlauto@polito.it*

been used to converge to the inverse problem solution. After that, the exponential growth of computational resources has allowed for an extensive use of more flexible and CPU consuming numerical approaches. Solvers based on FEM or FVM in two and three dimensions have been used to evaluate the thermal field, while, in the modelisation of the physics, the convection and radiation effects have been included. Then the research evolved to conjugate heat transfer analyses by including the mutual interactions with the fluid flow and by modelling film cooling effects [19]. From the optimization counterpart, the improvements of gradient based methods have lead to the various formulations by adjoint methods for 2D/3D problems [9, 17, 18], while the use of genetic algorithms has been also introduced for the solution of the single objective and multi-objective optimization problems.

A new impulse to thermal design in aerospace propulsion is related to recent efforts of designing aeroengines which meet the Vision 2020 requirements on gasturbine emissions and efficiency from Advisory Council for Aeronautics Research in Europe (ACARE). A straight way to enhance efficiency is obtained by increasing the maximum cycle temperature, i.e. the temperature into the combustion chamber. Moreover, other investigations introduce the Interstage Turbine Burner (ITB) concept to modify the thermodynamic cycle during flight, going towards variables cycle aeroengines. In both approaches a closer control of the temperatures is required and the thermal design of the some engine components, as the burners and the turbine blades, becomes more aggressive. In this scenario, automated inverse problem solvers can help the designer to make choices based on a wider investigation of the design variables space.

In the present work an approach to inverse problem solution is proposed. The method is based on the adjoint optimization and follows the footsteps of a technique of aerodynamic design [11],[12]. The mathematical treatment of the adjoint problem differs from previous adjoint approaches (e.g. see [9, 18]). In fact, the proposed formulation does not need a sensitivity problem to be solved and it includes a penalization for imposing geometrical constraints. To allow for the treatment of coated bladings, the heat conduction equation in a non-homogeneous material has been considered. As first step, circular cooling passages are treated and a way to impose non-intersecting contour constraints is developed. A FEM approach has been used both to compute the thermal field inside the turbine blade and to solve for the adjoint problem. The plan of the paper is as follows: in the next section the mathematical model and the inverse problem solution are presented; then the adjoint problem is derived and the numerical technique is explained. Finally the geometric parametrization of the blade cooling passages is derived and the procedure is validate against an analytical solution and against a test-case based on experimental data available in the open literature.

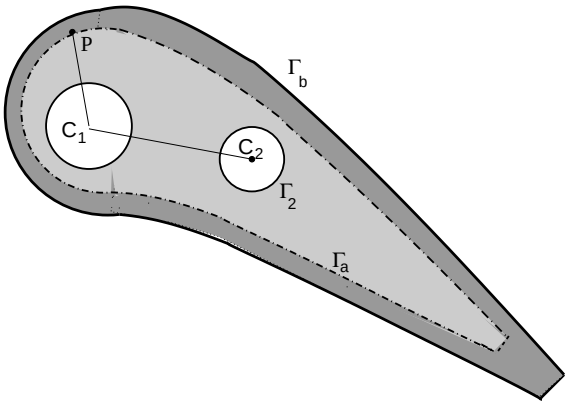

Figure 1: Domain geometry and nomenclature.

2 Governing Equations and Inverse Problem Formulation

Let consider the heat conduction equation in a non-homogeneous material and Robin boundary conditions. This set of equations may be written in a compact integral conservative form as:

$$\nabla \cdot (k \nabla T) = 0 \qquad on\ \Omega \tag{1a}$$

$$k \frac{\partial T}{\partial n} = h(T_g - T) \qquad on\ \Gamma = \Gamma_b \tag{1b}$$

$$k \frac{\partial T}{\partial n} = h(T - T_{cj}) \qquad on\ \Gamma_c = \bigcup_{j=1}^{N} \Gamma_j \tag{1c}$$

where T is temperature, T_g, T_{cj} are gas and coolant flows temperatures, h is the heat transfer coefficient and n is outward normal vector. For the thermal conductivity, we pose $k = k(\boldsymbol{x})$ as a function of position vector $\boldsymbol{x}$. In fact, in turbine blades with ceramic coating one can distinguish at least two regions with very different $k-$values. A sketch of a generic domain is given in Figure 1. Γ_b is the external surface of the turbine blade, Γ_a is the interfacial surface between inner core blade (light grey) and coating material (dark grey), and Γ_c is the union of the Γ_j surfaces of the N inner cooling passages. In the classical thermal inverse problem the boundary shape of the cooling passages Γ_j is regarded as unknown while some field variables are known at the external boundary Γ_b.
In the literature, whatever the method of solution used, various choices has been adopted in formulating the the inverse problem. In [7] both the heat flux and the temperature are imposed in a discrete set of points on Γ_b. In [8] the temperature on Γ_b is imposed and the geometry that realizes a target heat flux distribution in Γ_b is sought for. In [9] mixed boundary conditions are imposed in both Γ_b and on Γ_j, while looking for the geometry of the cooling passages that realizes the desired temperature in a discrete set on points on Γ_b. In the present work the approach is similar to the latter case, which is in our opinion the most suitable for a straight application, as well as for the experimental validation. We impose Robin boundary conditions both on the external blade surface Γ_b and on the internal cooling passages Γ_j, here supposed of circular shape, and we use adjoint based gradient method to find the hole locations and diameters which realize a desired temperature distribution $T_b(\boldsymbol{x})$ along the boundary Γ_b. In the present work the temperature distribution $T_b(\boldsymbol{x})$ is a known function related to a designer choice.
The numerical solution of system (1) is based on the Finite Element Method. The derivation of steady conduction equation is a standard exercise in classical textbook on FEM and will not repeated here. As a guidelines and using the terminology and notation of [21](see p.87–92), let assume for the temperature field the form

$$T(x, y) = \sum_{i=1}^{r} N_i T_i = [\boldsymbol{N}]\{\boldsymbol{T}\} \tag{2}$$

where $[\boldsymbol{N}] = \{N_1, N_i, \ldots, N_r\}$ is the shape function matrix and $\{T\} = \{T_1, T_i, \ldots, T_r\}^T$ the nodal temperature vector. The eqs. (1) can be reduced to

$$[\boldsymbol{K}]\{\boldsymbol{T}\} = \{\boldsymbol{f}\} \tag{3}$$

where

$$[\boldsymbol{K}] = \int_{\Omega} [\boldsymbol{B}]^T [\boldsymbol{D}][\boldsymbol{B}]\, d\Omega + \int_{\Gamma} h [\boldsymbol{B}]^T [\boldsymbol{N}] ds \tag{4}$$

$$\{\boldsymbol{f}\} = -\int_{\Gamma} q [\boldsymbol{N}]^T\, ds + \int_{\Gamma} h T_w [\boldsymbol{N}]^T ds \tag{5}$$

with

$$[\boldsymbol{B}] = \begin{bmatrix} \frac{\partial N_1}{\partial x} & \frac{\partial N_2}{\partial x} & \cdots & \frac{\partial N_r}{\partial y} \\ \frac{\partial N_1}{\partial y} & \frac{\partial N_2}{\partial y} & \cdots & \frac{\partial N_r}{\partial y} \end{bmatrix} \qquad [\boldsymbol{D}] = k(\boldsymbol{x})\, \boldsymbol{I} \tag{6}$$

The system (3) may be linear or not, depending on the expressions of $[\boldsymbol{K}]$ and $\{\boldsymbol{f}\}$. The parallel version of the SPOOLES package has been used to solve system (3).
The inverse problem is solved as an optimization problem, as outlined in the next section. The procedure iterates on a series of direct computations until all boundary condition and constraints are satisfied within an expected range of gradient and cost function residuals.

3 Variational formulation, adjoint equation and gradient

We define the cost function

$$\mathcal{F}(\Gamma_c, T) = \frac{1}{2}\int_{\Gamma_b} \left[T(\boldsymbol{x}) - T_b(\boldsymbol{x})\right]^2 d\Gamma + \chi\mathcal{P}(\Gamma_c) \tag{7}$$

where the $\mathcal{P}(\Gamma_c)$ is a penalization function added to enforce the geometric constraints to the optimization problem. The control variable is the set of relations defining the cooling passages geometry Γ_c. In two dimensions, each boundary has a parametric representation as follows

$$\Gamma_j \in R^2: \quad x = \sum_j \mu_j p_j(s), \qquad y = \sum_j \nu_j q_j(s) \tag{8}$$

where $p_j(s), q_j(s)$ are shape functions and μ_j, ν_j are the control parameters that can be packed in a single vector α_i.
The optimal temperature field must satisfy the governing equation (1) and some geometric constraints. In order to solve such constrained extremum problem we introduce the Lagrangian function

$$\mathcal{L}(T, \Gamma, \Lambda) = \mathcal{F}(\Gamma_c, T) + \int_\Omega \Lambda\, \nabla\cdot(\boldsymbol{k}\,\nabla T) d\Omega \tag{9}$$

where $\Lambda(\boldsymbol{x})$ is a Lagrange multiplier. The Lagrangian will allow us to treat the problem as unconstrained. A stationary configuration is found when the variation of $\mathcal{L}$ with respect to all its arguments, that are now considered independent functions, is 0. We compute $\delta\mathcal{L}$ as

$$\delta\mathcal{L} = \delta\mathcal{L}_T + \delta\mathcal{L}_\Lambda + \delta\mathcal{L}_{\Gamma_j} \tag{10}$$

All the contributions to $\delta\mathcal{L}$ must be 0 at the minimum. Hence, to find a stationary point we enforce

$$\delta\mathcal{L}_T = 0 \qquad \delta\mathcal{L}_\Lambda = 0$$

In general this results in $\delta\mathcal{L}_{\Gamma_j} \neq 0$. To reach the minimum we take $\delta\Gamma_j$ such that $\delta\mathcal{L} = \delta\mathcal{L}_{\Gamma_j} < 0$. Note that the variations of $\mathcal{L}$ with respect to the Lagrange multipliers Λ simply yield the heat conduction equation. The condition $\delta\mathcal{L}_T = 0$ leads to the adjoint equation and its boundary conditions. Based on the second Green's identity the second integral can be formulated as

$$\begin{aligned}
\delta\mathcal{L}_T &= \int_\Omega \Lambda\,\nabla\cdot(k\nabla(\delta T))d\Omega + \int_{\Gamma_b}(T-T_b)(\delta T)d\Gamma = \\
&= \int_\Omega (\delta T)\,\nabla\cdot(k\nabla\Lambda)d\Omega + \int_\Gamma \Lambda k\nabla(\delta T)\cdot\boldsymbol{n}\,d\Gamma - \int_\Gamma (\delta T)\,\boldsymbol{k}\,\nabla\Lambda\cdot\boldsymbol{n}\,d\Gamma + \int_{\Gamma_b}(T-T_b)(\delta T)d\Gamma = \\
&= \int_\Omega (\delta T)\,\nabla\cdot(k\nabla\Lambda)d\Omega + \int_{\Gamma_b}\left(\Lambda k\frac{\partial(\delta T)}{\partial n} - (\delta T)\,\boldsymbol{k}\,\frac{\partial\Lambda}{\partial n} + (T-T_b)(\delta T)\right)d\Gamma + \\
&\sum_i^N \int_{\Gamma_i}\left(\Lambda k\frac{\partial(\delta T)}{\partial n} - (\delta T)\,\boldsymbol{k}\,\frac{\partial\Lambda}{\partial n}\right)d\Gamma
\end{aligned} \tag{11}$$

By perturbing the boundary conditions (1b,1c) we can write

$$\begin{aligned} k\frac{\partial(\delta T)}{\partial n} &= -h(\delta T) \qquad && on\ \Gamma = \Gamma_b \\ k\frac{\partial(\delta T)}{\partial n} &= h(\delta T) \qquad && on\ \Gamma = \Gamma_j \end{aligned} \tag{12}$$

Substituting in (11) and considering all this integral contributions must vanish, we have

$$\begin{aligned} \nabla\cdot(k\nabla\Lambda) &= 0 \qquad && on\ \Omega \\ k\frac{\partial\Lambda}{\partial n} &= h\Lambda + (T - T_b) \qquad && on\ \Gamma_b \\ k\frac{\partial\Lambda}{\partial n} &= -h\Lambda \qquad && on\ \Gamma_j \end{aligned} \tag{13}$$

The adjoint problem (13) is formally identical to system (1). By changing $\Lambda \leftarrow T$ and with slight modifications to the set of boundary conditions, the numerical method used to solve the thermal problem can be applied to the adjoint problem.
To derive the variations $\delta\mathcal{L}_{\Gamma_j}$ we observe that, from eq.(8) they are formally equivalent to (and therefore replaced by) the variations of the Lagrangian function against the control parameters α_i

$$\delta\mathcal{L}_\alpha = \sum_i \frac{\partial}{\partial\alpha_i}\left[\int_\Omega \Lambda\nabla\cdot(k\nabla T)\,d\Omega + \chi\mathcal{P}\right]\delta\alpha_i = \sum_i \mathcal{G}_i\delta\alpha_i \tag{14}$$

where

$$\mathcal{G}_i = \frac{\partial}{\partial\alpha_i}\left[\int_\Omega \Lambda\nabla\cdot(k\nabla T)\,d\Omega + \chi\mathcal{P}\right] \tag{15}$$

The final expression of the terms $\mathcal{G}_i(\Gamma_i, T, \Lambda)$ depends on the adopted parametrization of the cooling passages geometry. The final formulation of $\mathcal{G}_i$ for circular cooling holes will be derived in the next section.
If we update α_i with

$$(\delta\alpha_i)^n = -\rho\mathcal{G}_i^n \tag{16}$$

by taking $\rho > 0$, then $\delta\mathcal{L}_\alpha \leq 0$. By iterating such a procedure, the minimum is eventually reached. This method, namely the Steepest Descent Method (SDM), has a slow convergence. Better convergence rates can be obtained with the Conjugate Gradient Method (CGM), in which the correction $\delta\alpha$ at the iteration n is given as

$$(\delta\alpha_i)^n = (\delta\alpha_i)^{n-1} + \beta^n\mathcal{G}_i^n \tag{17}$$

where β^n is defined by the modified Polak-Ribière formula

$$\beta^n = \max\left(\frac{\sum_i \mathcal{G}^n(\mathcal{G}^n - \mathcal{G}^{n-1})}{\sum_i \mathcal{G}^{n-1}\mathcal{G}^{n-1}},\ 0\right) \tag{18}$$

3.1 Geometric parametrization and constraints

Scope of this section is to derive a formulation of $\mathcal{G}_i$ able to parametrize the geometric optimization variables α_j and to include the necessary set of constraints.
We consider circular cooling passages. The boundary of each of M coolant passages is defined by

$$x = a_j + R_j\cos\theta, \qquad y = b_j + R_j\sin\theta \qquad 1 \leq j \leq M \tag{19}$$

where $C = (a_j, b_j), R_j$ are the center and radius of the j-th circle, respectively.
The vector of control variables can be defined as

$$\{\alpha\} = \{a_1, \ldots, a_j, \ldots, a_M, \quad b_1, \ldots, b_j, \ldots, b_M, \quad R_1, \ldots, R_j, \ldots, R_M\} \tag{20}$$

The holes boundaries cannot intersect each other and must lie far from the coating region of the blade. These requirements are constrains of the optimization problem and are introduced using penalization. In a way similar to [8], considering M coolant passages, we write the penalization function as

$$\mathcal{P} = \sum_{i}^{M} \frac{d_0}{A_i - d_0} + \sum_{j}^{M} \sum_{i=1, i\neq j}^{M} \frac{d_f}{B_{ij} - d_f} \tag{21}$$

where

$$A_i = \sqrt{(x_p - a_i)^2 + (y_p - b_i)^2} - R_i \tag{22}$$

is the minimum distance between the i-hole surface and the Γ_a contour (see Figure 1), and

$$B_{ij} = \sqrt{(a_i - a_j)^2 + (b_i - b_j)^2} - (R_i + R_j) \tag{23}$$

is the minimum distance between two coolant passage contours Γ_i and Γ_j. The complete set of derivatives is

$$\begin{aligned} \frac{\partial A_i}{\partial a_i} &= \frac{(a_i - x_p)}{\sqrt{(x_p - a_i)^2 + (y_p - b_i)^2}} \\ \frac{\partial A_i}{\partial b_i} &= \frac{(b_i - y_p)}{\sqrt{(x_p - a_i)^2 + (y_p - b_i)^2}} \\ \frac{\partial A_i}{\partial R_i} &= -1 \end{aligned} \tag{24}$$

and

$$\begin{aligned} \frac{\partial B_{ij}}{\partial a_i} &= -\frac{\partial B_{ij}}{\partial a_j} = \frac{(a_i - a_j)}{\sqrt{(a_j - a_i)^2 + (b_j - b_i)^2}} \\ \frac{\partial B_{ij}}{\partial b_i} &= -\frac{\partial B_{ij}}{\partial b_j} = \frac{(b_i - b_j)}{\sqrt{(a_j - a_i)^2 + (b_j - b_i)^2}} \\ \frac{\partial B_{ij}}{\partial R_i} &= \frac{\partial B_{ij}}{\partial R_j} = -1 \end{aligned} \tag{25}$$

Finally, we derive the expression for the variation of the Lagrangian function with respect to the parametrization.

$$\delta \mathcal{L}_\alpha = \sum_i \mathcal{G}_i \delta \alpha_i$$

Letting a variation $\alpha_i \leftarrow \alpha_i + \delta\alpha_i$, neglecting higher order terms, the functional $\mathcal{G}_i$ can be reduced to

$$\mathcal{G}_i = \begin{cases} \displaystyle\int_{\Gamma_i} \Lambda \nabla \cdot (k \nabla T) \frac{(x - \alpha_i)}{R_i} \, d\theta + \chi \frac{\partial \mathcal{P}}{\partial \alpha_i} & 1 \leq i \leq M \\ \displaystyle\int_{\Gamma_i} \Lambda \nabla \cdot (k \nabla T) \frac{(y - \alpha_i)}{R_{i-M}} \, d\theta + \chi \frac{\partial \mathcal{P}}{\partial \alpha_i} & M+1 \leq i \leq 2M \\ \displaystyle\int_{\Gamma_i} \Lambda \nabla \cdot (k \nabla T) r \, d\theta + \chi \frac{\partial \mathcal{P}}{\partial \alpha_i} & 2M+1 \leq i \leq 3M \end{cases} \tag{26}$$

where the derivative of the penalization function $\mathcal{P}$ are given by eqs.(24)-(25) . Finally, let note that in eq.(20) the three set of control variables a_j, b_j, R_j has been collected into a single vector α_i , therefore we are now led to a formulation of $\mathcal{G}_i$ in which the three different contributions have been distinguished.

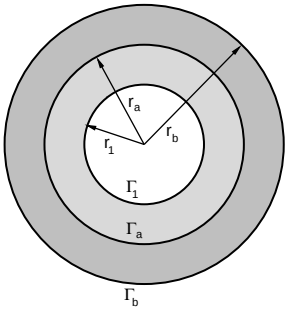

Figure 2: Test 1. Geometry

4 Numerical Results

The proposed numerical procedure is a classical optimization approach based on the adjoint equation to compute the functional gradient. Basically it consists of the following steps:

1. solve the direct problem (1)
2. solve the adjoint problem (13)
3. evaluate the functional gradient (14)
4. compute the conjugate direction of search via (17) and march towards the extremum
5. update the solution and test the convergence criterium

Two numerical applications are proposed in the next subsections. The first example is a test against an analytical solution. The second test is based on the experimental data of the Mark-II turbine blade [20] .

4.1 Coated cylinder with internal heating.

Let consider the heat transfer problem on a composite hollow cylinder with coating and a single circular heating passage as shown in Figure 2. The cylinder radii are $r_b = 58$, $r_a = 38$,$r_1 = 25$ millimeters. The inner flow has a temperature $T_c = 603.15\,K$, while the temperature of the external gas flow is $T_g = 303.15\,K$. The thermal conductivities of the inner core and of coating are $k_1 = 15$ and $k_2 = 0.2 \quad W/(Km)$, respectively.
Robin boundary conditions have been applied by specifying the heat convection rates for the inner flow passage ($h_c = 400\,W/m^2$) and for the exterior cylinder surface ($h_g = 60\,W/m^2$). The exact solution of the temperature field on the whole domain is obtained by classical analytical methods and it can be found in [13](page 63, example 3-11).
The inverse problem here proposed is inspired to a similar test-case found in [8]. From the knowledge of the temperature $T_b(\Gamma_b)$ on the external cylinder surface, the correct geometry of the system is sought. Starting from a generic geometric configuration for the cylinder, as shown in Figure 3, we solve for the location and radius of the inner hole that realizes the target wall temperature $T_w = T_b(\Gamma_b) \quad (= 337.230$ K) .

	a_1 [mm]	b_1 [mm]	r_1 [mm]	Q [W/m^2]	T_b [K]
Theoretical	0	0	25	2044.79	337.230
Numerical	0.303	0.012	24.933	2044.54	337.234
Error	$5.22{\cdot}10^{-3}$ (*)	$2.07{\cdot}10^{-4}$ (*)	0.27 %	0.012 %	0.0012 %

Table 1: Composite hollow cylinder Test. Comparison between numerical and theoretical value of main parameters. *In (*) the absolute error has been scaled to the external cylinder radius r_b.*

The problem parametrization follows the guidelines given in section 3.1. The control variables are

$$\alpha_i = \{a_1, b_1, R_1\}$$

i.e. the center coordinates and the radius of the inner circular hole, respectively. The thermal field and the related adjoint problem are then solved at each optimization step and the domain geometry is updated following eq. (17) by the CGM strategy. We used parabolic triangular finite element. Adaptive mesh refinement with error control is obtained by using the *bamg* meshing and adaptation tool [22]. Initial and final temperature field and geometry are shown in Figure 3. The system has shown a fast and monotonic convergence. In Figure 4 the control variables α_i and the functional residuals are plotted versus the optimization steps. As visible, after 20 iterations the functional residual is decreased of three orders of magnitude, even if a penalization has been applied. It must be noted, anyway, that there was very few control variables and that the influence of the penalty function was limited to the mitigation of asymmetric variations of the gradient components.
A comparison between numerical and analytical results is given in Table 1. The close agreement between data confirms the high resolution of the computations: the highest relative error is below 0.3%. We also note the remarkable accuracy of the heat flux computation, which involves a derivative evaluation and therefore was supposed to be more prone to numerical error. Moreover, the heat flux is a dependent variable which plays a key role on the system since it is imposed as boundary condition.

4.2 Mark II turbine blade

Experimental data about the Mark II and CF3X internally cooled turbine blades are available in the open literature [20] and have been used as a reference test-case in several work on the conjugate heat transfer and optimal blade design. The Mark II stator vane geometry is depicted in Figure 7b . The cooling system of this blade is composed by ten circular passages ($M = 10$). In the original work a method of evaluating the heat transfer coefficient is outlined and the experimental results (wall pressure, blade surface temperature and heat flux coefficient) are given for a wide range of working conditions. Walking on the footsteps of the previous section, the experimental data are used here to formulate a design problem and to solve it by the inverse numerical procedure. The measured surface temperature for a selected working condition (namely, the *run-15*) is assumed as target temperature $T_b(\boldsymbol{x})$. Then, starting from an arbitrary initial geometry, the correct coolant passage pattern is sought by solving the adjoint inverse problem.
First, we define the expression for the heat coefficients. For the coolant passages, the expression of the Nusselt number given in [20] is used

$$Nu_D = C_r \cdot 0.022\, Pr^{0.5} {Re_D}^{0.8} \tag{27}$$

where Pr and Re are the Prandtl and Reynolds numbers based on the coolant flow rate, viscosity and temperature. Cr is an empirical correction parameter introduced in [20].
For the external blade surface a polynomial approximation of the heat transfer coefficients has been computed by fitting and smoothing the experimental data. The curve obtained is shown in Figure 5. Again, the control variables are the centre coordinates and radii of the circular cooling passages. These variables has been packed as

$$\alpha_i = \{a_1, \ldots, a_j, \ldots, a_M, \quad b_1, \ldots, b_j, \ldots b_M, \quad R_1, \ldots, R_j, \ldots, R_M\} \qquad 1 \leq j \leq M$$

Starting from the generic initial condition depicted in Figure 7c, the inverse procedure has been applied until a satisfactory level of convergence is reached. The converged solution and temperature field are shown in Figure 7d, while the experimental and the evaluated blade surface temperature are compared in Figure 5 . The convergence of the objective functional and of the L^2-norm residual of controls α_i is monitored in Figure 6.
Although this test being quite severe (there are 30 control variables and strong penalty functions), the geometrical configuration obtained is close to the real one. For each α_i the relative error is less than 0.5%, a value slighly bigger than the error observed in the previous test T1.

It as also observed that the penalization effect is twofold: it reduces the convergence rate dramatically and it makes the solution less sensitive to the original objective functional. In the present case it acts also as a smoothing filter for the target temperature peaks and experimental noise. Nevertheless, by using a parallel implementation of the FEM code, the full computation has run in about one hour on a 8-core Intel i7 workstation.

5 Conclusions

An adjoint procedure for the solution of the inverse heat conduction problem has been proposed. Compared to similar approaches, the present method does not require the evaluation of an additional perturbation field and the functional gradient with respect to the controls variables is computed from its parametrization. This simplification is supposed to increase the robustness of the whole numerical procedure. The numerical tests carried out have shown an acceptable convergence rate, even if as much as 30 control variables and a strong penalization are taken into account. The latter is supposed to be responsible for the convergence worsening. In fact, it is well known that the number of control variables does not affect the performances of adjoint procedures. Nevertheless the computational cost is affordable on a medium level workstation.
The method has been specialized to the case of blade with circular passages holes. The extension to other geometries and to the three-dimensional case is straightforward but at the cost of 3D FEM computations and of a more complex parametric representation. The procedure has been validated against analytical and experimental solutions. From the numerical point of view a general purpose FEM engine can be used to solve both the thermal and the adjoint problem. Therefore, the method can be implemented in any free or commercial FEM engine that allows to impose user defined function as boundary conditions.
its optimality is of tb.

References

[1] Necati Özisik, M., Orlande, H. R. B., *Inverse Heat Transfer*. Taylor & Francis, London, 2000.

[2] Colaco, M. J., Orlande, Orlande, H. R. B., Dulikravich, G. S., Inverse and Optimization Problems in Heat Transfer, J. of the Braz. Soc. of Mech. Sci. & Eng., 28(1), p 1–24, 2006

[3] Szczygiel, I., Fic, A., Inverse Convection-Diffusion Problem of Estimating Boundary Velocity Based on Internal Temperature Measurements, Inverse Problems Eng., vol. 10, pp. 271-291, 2002.

[4] Beck,J.V., Blackwell, B. , St. Clair, C., *Inverse heat conduction: Ill-posed problems*, Wiley, New York, 1985.

[5] Alifanov, O.M. *Inverse Heat Transfer Problems*, Springer-Verlag, Berlin, 1994.

[6] Kurpisz, K., Nowak, A. J., Inverse Thermal Problems, Computational Mechanics Publications, Southampton, UK and Boston, 1995.

[7] Kennon, S. R., Dulikravich, G. S., The Inverse Design of Internally Cooled Turbine Blades, *ASME Journal of Engineering for Gas Turbines and Power*, Vol. 107, January 1985, pp. 123-126.

[8] Chiang, T. L., Dulikravich, G. S., Inverse Design of Composite Turbine Blade Circular Coolant Flow Passages, *ASME Journal of Turbomachinery*, Vol. 108, Oct. 1986, pp. 275-282.

[9] Huang, C. H., Hsiung, T. Y., An Inverse Design Problem of Estimating Optimal Shape of Cooling Passages in Turbine Blades, *Int. J. of Heat and Mass Transfer*, Vol. 42, 1999, pp. 4307-4319.

[10] Dulikravich, G. S., Martin, T.J., Inverse Design of Super-elliptic Cooling Passages in Coated Turbine Blades, Int. J. of Thermophysics and Heat Transfer, Vol. 8(2), 1994, pp. 288-94.

[11] Iollo, A., Ferlauto, M., Zannetti, L., An aerodynamic optimization method based on the inverse problem adjoint equations. J. Computational Physics, 173:87–115, 2001.

[12] Ferlauto, M., Iollo, A., Zannetti, L., Set of Boundary Conditions for Aerodynamic Design AIAA J., Vol. 42, No. 8, pp 1582–92, 2004.

[13] Necati Özisik, M., *Heat Transfer, a basic approach*. McGraw-Hill, London, 1985.

[14] Sarvari, S.M.H., Howell, J.R., Mansouri, S.H., Inverse Boundary Design Conduction-Radiation Problem in Irregular Two-dimensional Domains, Numerical Heat Transfer Part B, vol. 44, pp.209-224, 2003.

[15] Asokan, V., Narayanan, B., Zabaras,N., Stochastic inverse heat conduction using a spectral approach, Int. J. Numer. Meth. Engng, 60/7:1 (24), 2004.

[16] Taler, J., Duda, P., *Solving Direct and Inverse Heat Conduction Problems*, Springer, Berlin, 2006.

[17] Huang C. H., Chen, C. W., A boundary element based inverse-problem in estimating transient boundary conditions with conjugate gradient method, Int. J. Numer. Methods Engineering. 42 943–65,1998.

[18] Huang, C. H., Wang, S. P., A three-dimensional inverse heat conduction problem in estimating surface heat flux by conjugate gradient method Int. J. Heat Mass Transfer 42 ,1999.

[19] Montomoli, F., Adami, P., Martelli, F., A finite-volume method for the conjugate heat transfer in film cooling devices, Proc. IMechE Vol. 223 Part A: J. Power and Energy, 2009

[20] Hylton, L. D., Millec, M. S., Turner, E. R., Nealy, D. A. , York, R. E., Analytical and Experimental Evaluation of the Heat Transfer Distribution Over Surface of Turbine Vanes, NASA-Report CR 168015, 1983.

[21] Lewis, R. W. , Nithiarasu, P., Seetharamu, K. N., *Fundamentals of the Finite Element Method for Heat and Fluid Flow*, John Wiley & Sons Ltd,London, 2004.

[22] Hecht, F., Kuate, R., *Metric Generation for a Given Error Estimation*, Proceedings of the 17th International Meshing Roundtable, p.569–84, Garimella, Rao V. editors, Springer Verlag, 2008.

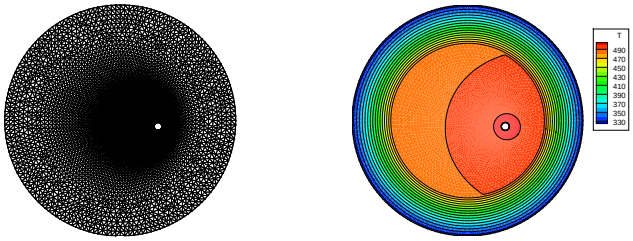

Initial configuration

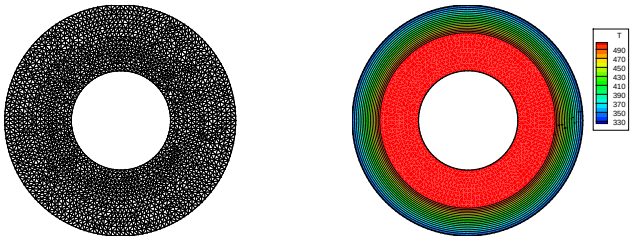

Final configuration

Figure 3: Test 1. Geometry and temperature field

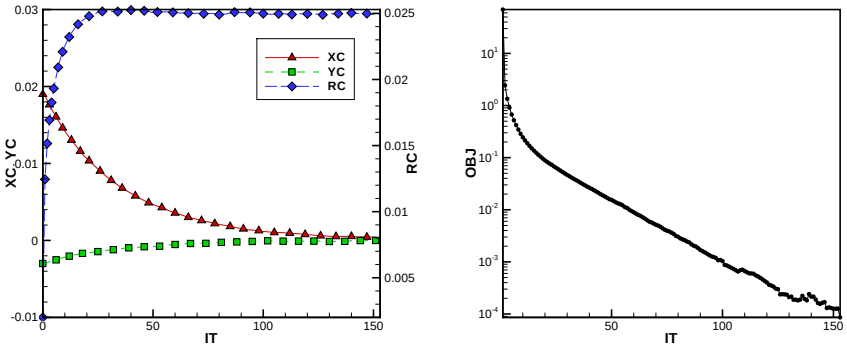

Figure 4: Test 1. Convergence history of $x_c = a1, Y_c = b1, R_c = r_1$ (left) and of the objective function residuals (right) versus optimization step.

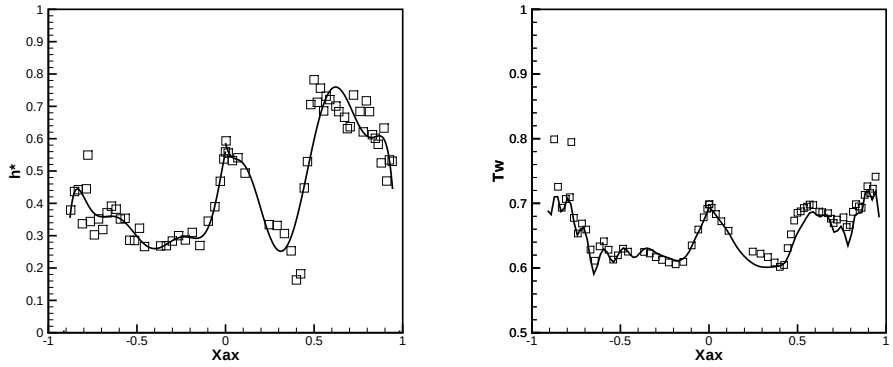

Figure 5: Test Mark II. Heat transfer Coefficient fitting (left) and comparison of the surface temperature obtained by the inverse problem and the target temperature distribution (right). Symbols refers to the experimental data, solid lines to numerical results).

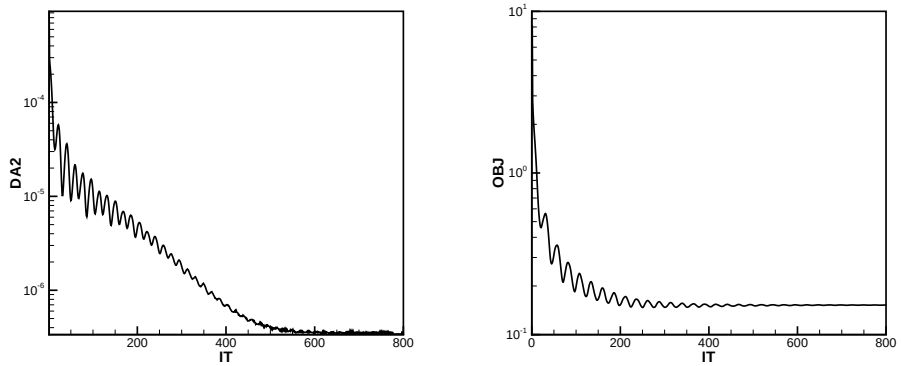

Figure 6: Test Mark II. Convergence history of L^2-norm of gradient residuals (left) and of the objective function residuals (right) versus optimization step.

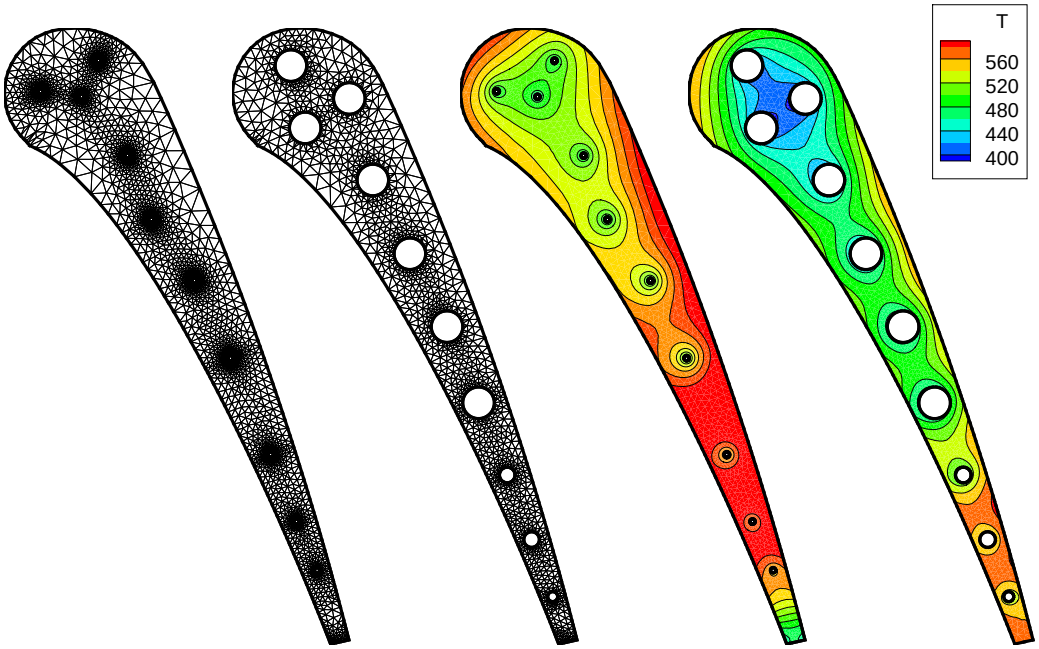

Figure 7: Test Mark II. Initial (a) and final (b) grid and cooling passage pattern. Initial (c) and final (d) temperature field.